Groundwater

Improved Lumped-Parameter and Numerical Modeling of Unsaturated Water Flow and Stable Water Isotopes

by Anne Imig[1,2], Fatemeh Shajari[1], Lea Augustin[1], Florian Einsiedl[1], and Arno Rein[1,2]

Abstract

Characterizing unsaturated water flow in the subsurface is a requirement for understanding effects of droughts on agricultural production or impacts of climate change on groundwater recharge. By employing an improved lumped-parameter model (LPM) approach that mimics variable flow we have interpreted stable water isotope data ($\delta^{18}O$ and $\delta^{2}H$), taken over 3 years at a lysimeter site located in Germany. Lysimeter soil cores were characterized by sandy gravel (Ly1) and clayey sandy silt (Ly2), and both lysimeters were vegetated with maize. Results were compared with numerical simulation of unsaturated flow and stable water isotope transport using HYDRUS-1D. In addition, both approaches were extended by the consideration of preferential flow paths. Application of the extended LPM, and thus varying flow and transport parameters, substantially improved the description of stable water isotope observations in lysimeter seepage water. In general, findings obtained from the extended LPM were in good agreement to numerical modeling results. However, observations were more difficult to describe mathematically for Ly2, where the periodicity of seasonal stable water isotope fluctuation in seepage water was not fully met by numerical modeling. Furthermore, an extra isotopic upshift improved simulations for Ly2, probably controlled by stable water isotope exchange processes between mobile soil water and quasi-immobile water within stagnant zones. Finally, although LPM requires less input data compared with numerical models, both approaches achieve comparable decision-support integrity. The extended LPM approach can thus be a powerful tool for soil and groundwater management approaches.

Introduction

The characterization of water flow in the unsaturated zone is an important task related to agronomics and environmental issues. Among others, this implies evaluating effects of climate change such as droughts on agricultural production, ecosystems, and groundwater recharge (Blanchoud et al. 2007; Woldeamlak et al. 2007; Kundzewicz and Döll 2009; Vrba and Richts 2015; Varis 2018). Further understanding and quantification of unsaturated flow is crucial for assessing the fate and transport of pollutants in the unsaturated zone and assessing their impacts on groundwater (Hsieh et al. 2001; Bradford et al. 2003; Dann et al. 2009; Stumpp et al. 2012).

In this context, laboratory experiments and inverse modeling approaches are used to determine soil hydraulic properties. Both have shortcomings; laboratory results may largely differ from those found at a field site, and additional uncertainties might occur from upscaling (Dinelli et al. 2000; Schwärzel et al. 2006; Winton and Weber 2018). For modeling approaches, detailed site data are required that often are not available, such as initial and boundary conditions (Asadollahi et al. 2020). Simplifying assumptions must be made, accordingly, which often bear considerable uncertainty.

As an alternative, if flow-related parameters such as soil moisture or hydraulic potentials are not available from field, environmental isotopes coupled with lumped parameter models (LPMs) can be used to obtain information on subsurface flow and relevant flow processes on

[1]Chair of Hydrogeology, TUM School of Engineering and Design, Technical University of Munich, Munich, Germany; anne.imig@tum.de

[2]Corresponding author: Chair of Hydrogeology, TUM School of Engineering and Design, Technical University of Munich, Arcisstr. 21, D-80333 Munich, Germany; +49 89 289 25869; fax: +49 89 289 25852; arno.rein@tum.de

Anne Imig and Fatemeh Shajari contributed equally to this work.

Article impact statement: Stable water isotopes combined with improved lumped-parameter and numerical modeling characterized flow in two vegetated lysimeters.

The authors declare no conflicts of interest.

Received December 2021, accepted August 2022.

doi: 10.1111/gwat.13244

the field scale (Leibungut et al. 2009). Comparing with numerical models, LPMs require only a limited number of data (tracer input and output) and fitting parameters ("lumped" parameters). Depending on the hydrological conditions, different tracer transport models, such as advection-dispersion, piston-flow, or exponential models, can be combined (Maloszewski and Zuber 1982; Maloszewski et al. 2002; Maloszewski et al. 2006; Einsiedl et al. 2009; Leibungut et al. 2009; Stumpp et al. 2009a; Stumpp et al. 2009b; Stumpp et al. 2009c; Stockinger et al. 2019).

The present study aims at addressing several disadvantages of LPMs and introducing an improved approach. Inherent to the LPM concept, steady-state flow is considered as a prerequisite of the implemented analytical solutions. Whereas this assumption is adequate for long-term groundwater conditions, it can be problematic for unsaturated flow where pronounced temporal variations often prevail. Our previous study (Shajari et al. 2020) revealed that the consideration of temporally varying flow conditions and tracer transport could potentially improve the simulation of stable water isotopes in seepage water and thus reduce uncertainties related to the fitted parameters. Therefore, in the present study, we have extended the LPM approach and subdivided the whole simulation time into several sub-periods for mimicking transient flow. In this way, each set of parameters (mean transit time and dispersion parameter) is fitted for each sub-period. To this respect, Maloszewski et al. (2006) considered a yearly changing mean transit time for simulating stable water isotope transport in different lysimeters. Stumpp et al. (2007, 2009a, 2009b) extended this approach by varying the dispersion parameter, in addition to mean transit time, and obtained improved model prediction.

Further, to better describe short time fluctuation and measured peaks we extend the traditional LPM approach by implementing a dual-permeability system (separation of transport through subsurface matrix and along preferential flow paths) and consideration of possible contribution of immobile water. The importance of preferential flow on adequately characterizing unsaturated zone flow and transport processes has been studied intensively by Stumpp et al. (2009c), Isch et al. (2019), Benettin et al. (2019), and Radolinski et al. (2021). The combination of LPM and preferential flow has successfully been applied by Stumpp et al. (2007) and Shajari et al. (2020).

Another difficulty of LPM models is the adequate description of the tracer input function (McGuire et al. 2002; Maloszewski et al. 2006; Stumpp et al. 2009a, 2009b, 2009c). We have considered different input functions to account for seasonal or vegetation-related variation and different assumptions for evapotranspiration (Shajari et al. 2020). To the best of our knowledge, only few lysimeter studies with stable water isotopes are available that consider the same vegetation for different soil types.

In this article, we applied an extended LPM approach in two lysimeters filled with different soils (sandy gravels and clayey sandy silt) and vegetated by maize. We also carried out numerical simulations of water flow and stable water isotope transport (using HYDRUS-1D) to verify the extended LPM approach.

Materials and Methods

Lysimeter Study Site and Considered Soils

Field studies were done at two weighable lysimeters as described in detail by Shajari et al. (2020). These lysimeters are located near Wielenbach, Germany, about 48 km southwest of Munich (elevation 549 m above sea level). They consist of stainless-steel cylinders filled with undisturbed soil cores (surface area of 1 m^2, length of 2 m). Lysimeter 1 (Ly1) contains sandy gravels (taken from a former target shooting area near Garching, Germany), Lysimeter 2 (Ly2) contains clayey sandy silt (taken from an agricultural site at Hutthurm-Auberg near Passau, Germany). The soil of Ly1 is characterized as a calcaric Regosol (according to the Word Reference Base for Soil Resources, WRB 2015). It has developed above sandy to silty calcareous gravels, where four distinct soil layers were identified. The soil of Ly2 is a Cambisol (Stagnosol) (WRB 2015) developed above gneiss, which was sub-divided into five layers. Table S1 contains information on soil horizons and measured grain size distributions (only limited data available for Ly1). The lysimeters were vegetated with maize (upper boundary) and had seepage face controlled lower boundaries, allowing drainage if the soil is saturated but no upward water inflow.

Observations and Sampling at the Study Site

Precipitation, seepage water, and lysimeter weight were recorded automatically as described in detail by Shajari et al. (2020). Precipitation data prior to 2013 were collected at a meteorological weather station at the lysimeter study site. Samples for stable water isotope analysis were collected from July 2013 to April 2016 on a weekly basis, with greater intervals during dry season and smaller intervals during wet season. Stable water isotopes ($^2H/^1H$, $^{18}O/^{16}O$) were analyzed using laser spectroscopy (details are given in Shajari et al. 2020). From measured isotope contents, delta-values ($\delta^{18}O$ and δ^2H) were calculated as $\delta\ (‰) = (R_{Sample} - R_{Standard})/R_{Standard} \times 1000$, with stable water isotope ratio R ($^2H/^1H$ or $^{18}O/^{16}O$) as the sample (R_{Sample}) and the Vienna Standard Mean Ocean Water (V-SMOW) as the standard ($R_{Standard}$). The analyzer showed a precision of 0.1‰ for $\delta^{18}O$ and 0.5‰ for δ^2H. Measurements or sampling within the soil cores, such as of water content or hydraulic potential, were not possible due to experimental restrictions.

Soil Sampling and Measurement of Soil Hydraulic Parameters

Unfortunately, the original sites where the soil cores were taken are not accessible anymore, due to infrastructure. Consequently, for Ly1, soil samples were taken about 1 km West of the original excavation

site for the soil core (near Garching, Germany), where soil types and textures are assumed similar. Three replicated soil samples were taken at a fresh hillside cutting from three depths (0–0.1 m, >0.1–0.2 m, and 1.0–1.2 m below surface, cf. Table S2). For these samples, water retention curves and unsaturated hydraulic conductivity were measured using the ku-pF apparatus DT 04-01 (Umwelt-Geräte-Technik GmbH UGT, Germany). Measurements yielded the following soil hydraulic parameters (SHPs): residual and saturated soil water content (θ_r and θ_s), water retention curve shape parameters α and n (van Genuchten–Mualem model) and saturated hydraulic conductivity K_S (cf. Table S2). For Ly2, soil sampling at a representative site was not possible due to restricted accessibility.

Lumped-Parameter Modeling

We have used LPM to simulate the transport of stable water isotopes ($\delta^{18}O$, $\delta^{2}H$) in the lysimeters. LPM simulate tracer transport in the unsaturated zone by solving a convolution integral that includes tracer input and the tracer transfer function (also called weighing function). If tracer transport through the subsurface matrix and along preferential flow paths are considered, the following equation can be applied (Maloszewski and Zuber 1982; Stumpp et al. 2007; Shajari et al. 2020):

$$C_{\text{out}}(t) = (1 - p_{\text{PF}}) \int_0^t C_{\text{in}}(t-\tau) g_M(\tau)\, d\tau + p_{\text{PF}} \int_0^t C_{\text{in}}(t-\tau) g_{\text{PF}}(\tau)\, d\tau \quad (1)$$

where C_{out} and C_{in} are tracer output and input concentration as a function of time, respectively, and are delta values (‰) of seepage (lysimeter outflow) and recharging water ($\delta^{18}O$ and $\delta^{2}H$) in this study. g_M and g_{PF} are transit-time distribution functions for the subsurface matrix and preferential flow paths (−), respectively, and τ indicates all possible transit times within the system (d). The first term on the right-hand side of Equation 1 describes tracer transport through the soil matrix, while the second term describes transport along preferential flow paths; p_{PF} denotes the portion of preferential flow (−). Advective-dispersive tracer transport was considered for the subsurface matrix (Lenda and Zuber 1970; Kreft and Zuber 1978),

$$g_M(\tau) = \frac{1}{\tau\sqrt{4\pi P_D \tau/T}} \exp\left[-\frac{(1-\tau/T)^2}{4P_D\tau/T}\right] \quad (2)$$

while pure advection (piston flow) was assumed for tracer transport along preferential flow paths (Maloszewski and Zuber 1982),

$$g_{\text{PF}}(\tau) = \delta(\tau - T_{\text{PF}}) \quad (3)$$

where T is mean transit time (or mean travel time) of water (day), and P_D is the dispersion parameter (−). T_{PF} is the mean residence time of water within preferential flow paths, which was set to the temporal resolution for modeling (day). Fitting parameters for lumped modeling are thus T, P_D, and p_{PF}. For the consideration of tracer transport through the subsurface matrix only, p_{PF} is set to zero.

The sampling interval for the isotope data depended on seepage water availability and varied between 1 day and 2 weeks (in average weekly). Hence for the LPM simulation a time step of 1 day was chosen.

The recharge of stable water isotopes into the unsaturated zone as a function of time was not measured directly, but estimated from measured stable water isotopes of precipitation. Two different assumptions for the input function were compared (IF0, IF2), as described by Shajari et al. (2020). In summary, IF0 considers precipitation as input (no modification) and IF2 considers weighting over hydrologically relevant time periods and actual evapotranspiration determined from the water balance at the lysimeters. Weighting periods of 1, 3, and 6 months were used to account for short-term effects as well as for seasonal and vegetation-related variations of recharge (based on Grabczak et al. 1984 and Maloszewski et al. 1992, similarly applied by Stumpp et al. 2009a and 2009b, and Shajari et al. 2020). The consideration of 6-month periods, that is, summer (maize growth, April to September) and winter (October to March), yielded best model curve fits in our previous study (Shajari et al. 2020). Thus, in the present study, we also applied this summer–winter scheme for setting up six sub-periods for the observation time at the lysimeters. The final sub-period was extended from March to April 2016 as measurements ended afterwards. For each lysimeter, it was required to consider a pre-phase prior to the observations period, to ensure complete simulated tracer breakthrough. Based on analytical modeling, pre-phases of 1 year for Ly1 and 5 years for Ly2 revealed adequate (cf. section Pre-phase setup in Appendix S1). Eight sub-periods were considered for Ly1 (for July 2012 to April 2016) and nine for Ly2 (initial sub-period P1 for July 2008 to June 2012). Thus, eight parameters of T, P_D, and p_{PF} for Ly1 and nine for Ly2 were fitted.

Numerical Modeling

Unsaturated flow

Unsaturated flow of the studied lysimeter soil cores was simulated numerically with the software package HYDRUS-1D, which solves the Richards equation (Šimůnek et al. 2008). The van Genuchten–Mualem model was applied for the soil hydraulic functions $\theta(h)$ and $K(h)$ (van Genuchten 1980 and Mualem 1976, respectively):

$$\theta(h) = \begin{cases} \theta_r + \frac{\theta_s - \theta_r}{[1+|\alpha h|^n]^m} & \text{if } h < 0 \\ \theta_s & \text{if } h \geq 0 \end{cases} \quad (4)$$

$$K(\theta) = K_s S_e^l \left[1 - \left(1 - S_e^{1/m}\right)^m\right]^2 \quad (5)$$

where $\theta(h)$ and $K(\theta)$ are water content ($L^3\ L^{-3}$) and hydraulic conductivity ($L\,T^{-1}$) as a function of hydraulic pressure head h (L); θ_r and θ_s are the residual and saturated water content, respectively (L^3L^{-3}), and K_s is the saturated hydraulic conductivity (LT^{-1}). α, n, and m are empirical water retention curve shape parameters, where $m = 1 - 1/n$ $(n > 1)$ (−). α is often related to the inverse air-entry suction (L^{-1}), whereas n to the pore-size distribution (−). The effective saturation S_e is given as $S_e = (\theta(h) - \theta_r)/(\theta_s - \theta_r)$ (−). The pore connectivity factor l represents the tortuosity of transport paths within the system (−). To decrease the number of fitting parameters, it was set to 0.5 as proposed by Mualem (1976).

Stable water isotope transport in the unsaturated zone

Solute transport can be described by the advection-dispersion equation for the unsaturated zone as follows (Fetter 1993):

$$\frac{\partial(\theta C)}{\partial t} = \frac{\partial}{\partial z}\left(\theta D \frac{\partial C}{\partial z}\right) - \frac{\partial(qC)}{\partial z} \tag{6}$$

where C is the tracer concentration ($M\,L^{-3}$), D is the dispersion coefficient ($L^2\ T^{-1}$), and q is the volumetric fluid flux ($L\,T^{-1}$). In this study, for the transport of stable water isotopes, only longitudinal dispersion is considered. D is defined as $D_L = \alpha_L \cdot v$, where α_L is the longitudinal dispersivity (L), while v represents flow velocity ($L\,T^{-1}$). The dispersion parameter P_D can be calculated as $P_D = \alpha_L/x$ (−), where x is the flow length (L) ($x = 2$ m, representing lysimeter length).

For stable water isotope transport modeling with HYDRUS-1D, a modified approach developed by Stumpp et al. (2012) was used. In the standard version of HYDRUS-1D, evaporation leads to an accumulation of solutes at the upper boundary. The modified code contains changes for the upper boundary so that evaporation has no effect on isotope content (Stumpp et al. 2012). Thus, isotopic fractionation due to evapotranspiration is neglected. This is expected to be a valid assumption if the observed regression line of stable isotopes of soil water is very close to the local meteoric water line (LMWL) of precipitation (Stumpp and Hendry 2012). As reported by Shajari et al. (2020), such a similarity was also observed at our study site.

Consideration of preferential flow paths and the influence of immobile water

To account for the presence of a second permeability system, we considered preferential flow paths for numerical modeling. This was done outside of HYDRUS-1D, since currently available HYDRUS-1D approaches cannot simulate stable water isotopes in a dual permeability domain. As a simplified assumption, similar to lumped-parameter modeling, piston flow (advective transport) was assumed for the preferential flow paths. A portion of precipitation (p_{PF}) directly enters preferential flow paths, and the remaining portion ($1 - p_{PF}$) reaches the surface of the subsurface matrix. Mean residence times of preferential flow T_{PF} between 1 and 7 days were considered. Information on preferential flow is restricted by the temporal resolution of measurements, which was 1 week in average (upper boundary), and modeling was carried out on a 1-day resolution basis (lower boundary; cf. Shajari et al. 2020). The model setup is illustrated in Figure S1. Calculations were done using a Python script, coupled to HYDRUS-1D executables and input files.

Furthermore, we have extended the model approach by including an additional isotopic component that accounts for the mixing of mobile and immobile water. As a simplified assumption, a constant positive delta-value is added to represent the influence of immobile water that is isotopically enriched.

Numerical model setup

For numerical modeling, the soil cores of the two lysimeters (Ly1 and Ly2) are represented by 1D model domains, and each model domain is discretized in 200 model cells with uniform cell size of 1 cm. As initial guess, SHPs for grain size distributions similar to Ly2 were obtained from the Rosetta data base. For Ly1, experimentally measured SHPs were available. For the diffusion coefficient in free water, a value of 10^{-9} m^2/s was used (Stumpp et al. 2012; Stumpp and Hendry 2012).

For water flow, the upper boundary was set as an atmospheric boundary condition with surface layer, and seepage face ($h = 0$) was applied to the lower boundary (lysimeter outflow). At the upper flow boundary, we specified measured precipitation and actual evapotranspiration (ET) determined from the water balance at the lysimeters, as described in detail by Shajari et al. (2020). HYDRUS-1D was modified to estimate actual ET by setting h_{CritA} (the minimum allowed pressure head) to −1,500,0000 cm as applied by Groh et al. (2018). For tracer transport simulation, a time-variable solute flux boundary was applied at the top, and a zero-concentration gradient was applied at the bottom.

Since positive delta-values are required for transport modeling in HYDRUS-1D, a constant offset (23‰) was added to the (negative) delta-value input and the offset was subtracted again from the modeling results (Stumpp et al. 2012; Sprenger et al. 2016).

For modeling the pre-phase, a pressure head of −340 cm (i.e., water content of field capacity) was set as the initial condition for the entire soil column. A modeling pre-phase of 2.5 years was considered for Ly1 (January 2011 to June 2013) and 5.5 years for Ly2 (January 2008 to June 2013) prior to the observation period for allowing the pore volume to exchange at least one time. Stable water isotope input for the modeling pre-phase was obtained from the meteorological station near Passau–Fürstenzell (as no measurements were available at lysimeter site; cf. Figure S2). Initial stable water isotope content was set to an arbitrary value of 2‰ at all depths.

Table 1
Ly1: Parameter Values Fitted From Lumped-Parameter Modeling With Different Input Functions (IF) and Statistics

	S12	W12/13	S13	W13/14	S14	W14/15	S15	W15/16	Av.	R^2 (−)	RMSE (‰)	ME (‰)
Traditional LPM, input function IF0												
T (day)									129	0.48	1.51	−0.61
P_D (−)									0.7			
Input function IF0												
T (day)	121	118	135	145	98	119	165	138	131			
P_D (−)	0.14	0.14	0.08	0.14	0.10	0.09	0.05	0.05	0.10	0.86	0.81	−0.43
p_{PF} (%)	14	9	14	14	13	10	15	12	13			
Input function IF2, 1 m												
T (day)	121	88	117	139	112	121	176	135	126			
P_D (−)	0.13	0.13	0.10	0.14	0.14	0.11	0.07	0.05	0.11	0.87	1.08	−0.79
p_{PF} (−)	7	6	12	9	10	8	12	8	9			
Input function IF2, 3 m												
T (day)	100	95	115	149	122	119	177	138	127			
P_D (−)	0.13	0.08	0.10	0.16	0.13	0.09	0.07	0.05	0.10	0.87	1.06	−0.63
p_{PF} (%)	7	6	8	6	12	6	12	7	8			
Input function IF2, 6 m												
T (day)	100	91	111	152	122	119	178	138	126			
P_D (−)	0.13	0.08	0.10	0.14	0.14	0.09	0.07	0.05	0.10	0.89	1.03	−0.67
p_{PF} (%)	8	7	12	6	10	6	12	7	9			

Note: Traditional LP: values taken from Shajari et al. (2020).
Abbreviations: Av., average value for the whole time period; S, summer, W, winter.

Estimation of median transit times

Following Sprenger et al. (2016), ideal virtual tracers were injected every day (constant amounts) at the top of the unsaturated zone, and cumulative tracer breakthrough curves were calculated based on modeled concentration with HYDRUS-1D. For each of those curves, the time when median concentration occurred was considered the individual median transit time (MTT).

Model Curve Fitting Procedure

Least-square fitting of predictions to observations was done by manual expert adjustment of model parameters, in an iterative procedure. This was based upon statistical evaluation of curve fits using the root mean square error (RMSE), mean error (ME), and coefficient of determination (R^2) (Stumpp et al. 2009a). For lumped-parameter modeling, $\delta^{18}O$ in seepage water was set as objective function. In an iterative procedure, a set of T, P_D, and p_{PF} was first fitted for the whole modeling period, then fitted for yearly and finally fitted for the seasonal (winter/summer) periods.

For numerical modeling, the hydraulic and transport parameters were inversely calibrated by using the model-independent parameter estimation utility PEST developed by Doherty (2020). Measured delta values in lysimeter outflow, drainage, and water content changes (estimated from recorded lysimeter weight) were used as objective functions (calibration targets). Details on parameter bounds for the fitting procedure are provided in Table S3. Transport of both $\delta^{18}O$ and $\delta^{2}H$ was simulated, yielding very similar fitting parameters. In the following, results for $\delta^{18}O$ are presented in detail.

Results and Discussion

Lumped-Parameter Modeling

Applying the extended LPM approach with temporally varying flow conditions substantially improved the model fit. For Ly1, R^2 was improved from 0.48 (traditional LPM) to 0.86 (IF0, Table 1) and for Ly2, R^2 was improved from 0.19 (traditional LPM) to 0.39 (IF0, Table 2). Underestimations were reduced significantly, for Ly1 in particular for the first year and for the final part of the curve (third peak starting in June 2015) (Figure 1a) and for Ly2 especially for the first year and the third peak (May to November 2015) (Figure 2a).

Application of the extended LPM approach revealed pronounced seasonal variations (winter-summer) and annual differences of model parameters (Tables 1 and 2 and Figure 3). In addition, basic statistical data of measured $\delta^{18}O$ in Ly1 and Ly2 as well as seasonal variations are summarized in Table S4 and Figure S3.

The fitted parameters for this study are within a typical range for similar soils (discussed in detail in Shajari et al. 2020). As shown in Figure 3d and 3e for Ly 1 and Figure 3j and 3k for Ly2, neither T nor P_D variation revealed a clear pattern with respect to the season (values given in Table 1). For a sandy gravel soil, Stumpp et al. (2009b) found seasonal variations of T and P_D between 182–413 days and 0.09–0.14, respectively,

Table 2
Ly 2: Parameter Values Fitted From Lumped-Parameter Modeling With Different Input Functions (IF) and Statistics

Par.	P1	S12	W12/13	S13	W13/14	S14	W14/15	S15	W15/16	Av.	R^2 (−)	RMSE (‰)	ME (‰)
Traditional LPM, input function IF0													
T (day)										362	0.19	0.67	−0.05
P_D (−)										1.2			
Input function IF0													
T (day)	350	370	300	360	430	320	380	300	375	354			
P_D (−)	0.7	0.7	0.8	0.5	0.8	0.5	0.9	0.4	0.8	0.7	0.39	0.73	−0.09
p_{PF} (%)	7	8	7	6	10	9	8	12	12	9			
Input function IF2, 1 m													
T (day)	350	350	300	350	445	310	370	330	375	354			
P_D (−)	0.7	0.7	0.8	0.7	0.8	0.5	0.7	0.4	0.6	0.7	0.38	0.68	−0.30
p_{PF} (%)	7	8	8	4	11	10	8	12	11	9			
Input function IF2, 3 m													
T (day)	350	350	300	390	445	310	370	330	385	360			
P_D (−)	0.7	0.7	0.8	0.7	0.7	0.4	0.7	0.3	0.5	0.6	0.40	0.60	−0.11
p_{PF} (%)	7	8	8	3	9	11	8	7	11	8			
Input function IF2, 6 m													
T (day)	350	350	305	365	445	330	390	310	390	361			
P_D (−)	0.7	0.7	0.8	0.6	0.7	0.5	0.9	0.4	0.7	0.7	0.40	0.64	−0.23
p_{PF} (%)	7	9	8	3	9	6	5	7	6	7			

Note: P1: additional modeling pre-phase, July 2008 to June 2012.

where a clear trend of summer–winter oscillation seems not obvious. Parameter variations from year to year, found in the present study, are within a similar range as observed by Stumpp et al. (2009b) and Maloszewski et al. (2006) for different soils.

Modification of the input function led to further modeling improvements. For Ly1, IF2 with 6-month weighting showed the best fit (Table 1 and Figure 1b) and for Ly2 IF2 with 3- and 6-month weighting (Table 2 and Figure 2b). The modified input function considers weighted input and thus reflects seasonal changes on a 3- and 6-month basis as well as shorter (1-month) fluctuations of infiltration.

The implementation of preferential flow paths further improved simulations (cf. Figure 1c and Table 1 for Ly1 and Table 2 and Figure 2c for Ly2). Rapid transport of recharging $\delta^{18}O$ along preferential flow paths can explain the observed short-term fluctuations of $\delta^{18}O$ in seepage water. Accordingly, p_{PF} tends to be increased when the precipitation rate is high (see Figure 3f vs. Figure 3c for Ly1, Figure 3l vs. Figure 3i for Ly2). Such a dependency was also found by Stumpp et al. (2007). In contrast, no clear season-dependency of p_{PF} can be seen for Ly2. The difference between the lysimeters could possibly be explained by different contributions of preferential flow paths. For many soils, as found for Ly1 (with some exceptions), contributions of preferential flow tend to be higher in summer (Täumer et al. 2006; Demand et al. 2019). This can be explained by low water contents (that prevail during extended dry periods) and events of high precipitation (Demand et al. 2019).

Gazis and Feng (2004) studied the isotopic composition of precipitation and soil water in sandy loam soils. Their observations suggest that the mixing of percolating water with immobile water can lead to higher $\delta^{18}O$ values (due to the prevalence of isotopically heavy summer water), as observed in our study for Ly2. This finding supports our assumption of a "constant upshift" of modeled isotope values in the seepage water of Ly2, for mimicking contributions of immobile water. A $\delta^{18}O$ upshift of 1 ‰ was found as a best fit. In contrast, mixing between mobile and quasi-immobile water might have a lower influence for the seepage water of Ly1 (no upshift was required there). This might be due to the finer pore structure and thus as a higher effective soil water volume in Ly2 (cf. Shajari et al. 2020). Consideration of the constant isotopic upshift within the LPM did not impact values of T, P_D, and p_{PF}.

As a major change to our previous study (Shajari et al. 2020), we have considered a longer modeling pre-phase of 5 years (instead of 1 year) for LPM modeling of Ly2. This was done both for constant flow (dashed curve in Figure 2a) and varying flow (other model curves in Figure 2). This longer pre-phase revealed to be more adequate given the finer-grained structure and higher mean travel time of water within Ly2 (details given in section Pre-phase setup in Appendix S1).

Numerical Flow and Stable Water Isotope Transport Modeling

As shown in Figure 4a, the modeled curves describe the observed behavior of $\delta^{18}O$ for Ly1 well, reproducing seasonal periodicity. As found above for lumped-parameter modeling, the application of stable water isotope transport along preferential flow paths resulted in slightly better overall curve fits. Portions of preferential

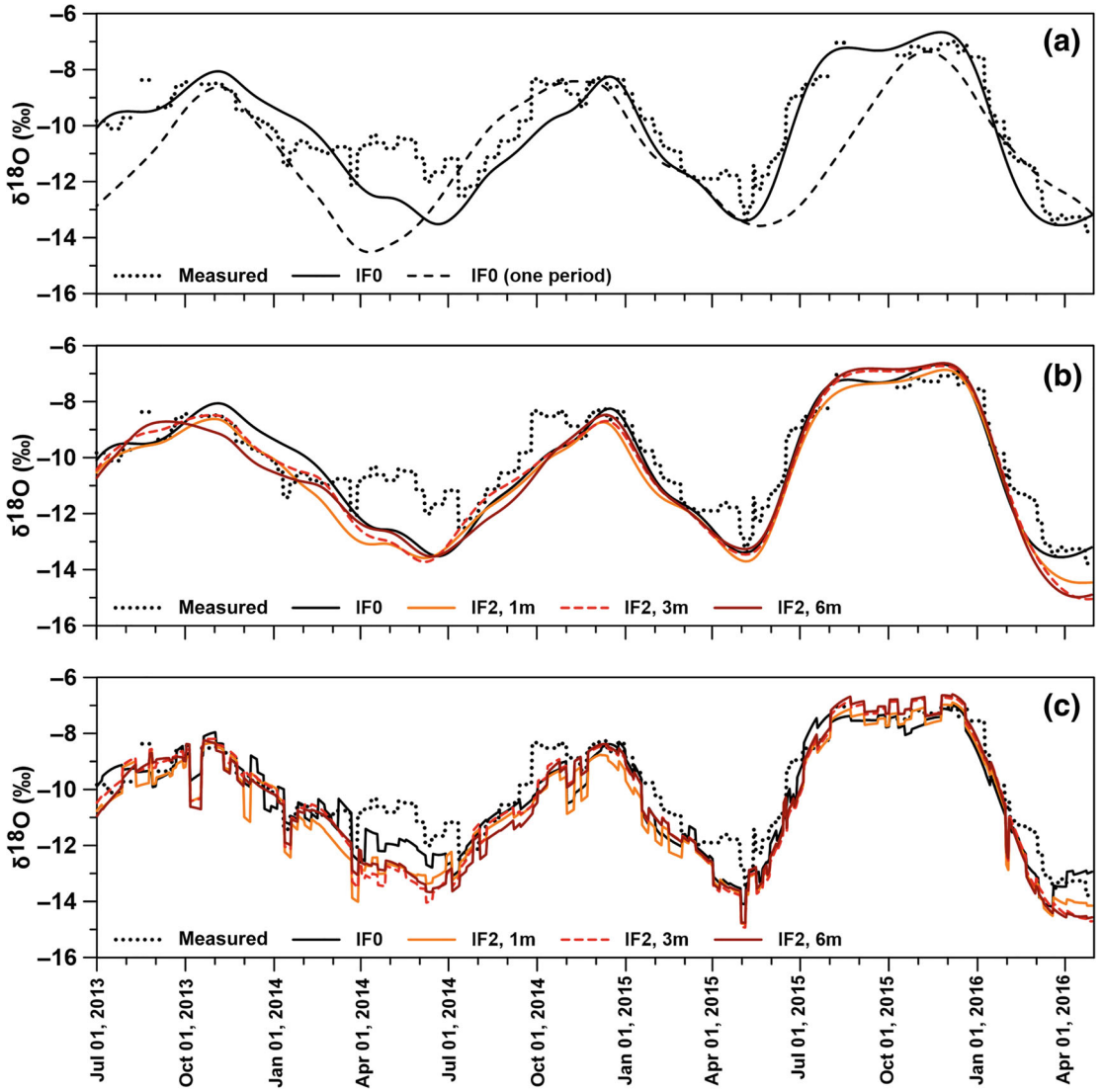

Figure 1. Measured and modeled (lumped-parameter model, LPM) $\delta^{18}O$ in the seepage water of Ly1 as a function of time. (a) Modeling with input function IF0 ($\delta^{18}O$ of precipitation as input), considering variable flow (extended LPM, eight subperiods) and constant flow ("traditional" LPM, one period). (b,c) Modeling with input function IF2 and weighted input within 1, 3, and 6 months (1, 3, and 6 m), considering variable flow. (a,b): stable water isotope transport through the subsurface matrix flow, only; (c): transport through the matrix plus along preferential flow paths.

flow p_{PF} of 8–11% led to similarly good model curve fits, with mean residence times of water within preferential paths (T_{PF}) of 6–7 days. This rather wide range of p_{PF} and T_{PF} indicates a low sensitivity of preferential flow characteristics. This could possibly be explained by the coarse texture of the soil of Ly1, which is characterized by sandy gravels. Connected pores may act as preferential flow paths (enabling rapid transport of the infiltrating water).

For Ly1, fitted values of saturated water content θ_s and dispersion parameter P_D (Table 3) are within typical ranges found for sandy gravels (Stumpp et al. 2009b; Sprenger et al. 2015) (Table 3 and simulated soil water retention curves shown in Figure S5). For saturated hydraulic conductivity K_S, fitted values match those found by Stumpp et al. (2009c) and Freeze and Cherry (1979).

Results of numerical modeling for Ly2 are shown in Figure 4b. As for LPM application, modeled curves were shifted up by a constant value (0.8‰). This value is slightly higher than that found from LPM application (1‰) and corresponds to a second component that contributes to delta values in seepage water. The seasonal periodicity seems not fully matched by the simulation. The consideration of preferential flow (Figure 4b) substantially improved simulation and reduced under- and overestimations. Moreover, short-term fluctuations were better described (cf. Table 3 for statistical evaluation of curve fits with preferential flow). The fitted saturated water content θ_s of 0.28 appears to be at the lower end of frequently reported ranges around 0.3–0.5 (Table 3 and simulated soil water retention curves shown in Figure S5). This could possibly be explained by the relatively high contents of sand (cf. Table S1) together with a poor sorting of

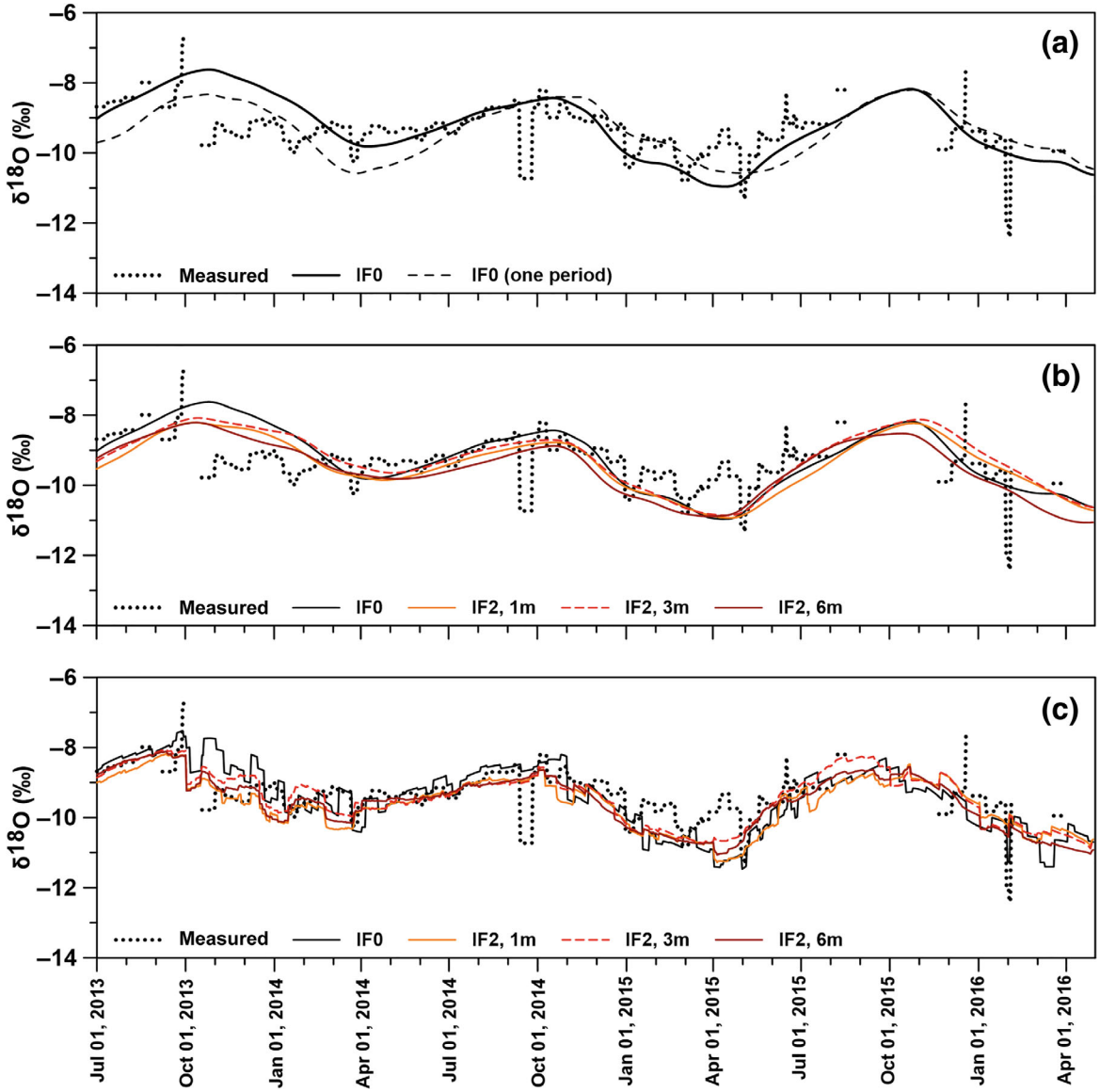

Figure 2. Measured and modeled (lumped-parameter model, LPM) $\delta^{18}O$ in the seepage water of Lysimeter 2 as a function of time. (a) Modeling with input function IF0 considering variable flow (extended LPM, nine sub-periods) and constant flow ("traditional" LPM, one period). (b,c) Modeling with input function IF2 and weighted input within 1, 3 and 6 months (1 m, 3 m, 6 m), variable flow. (a,b): stable water isotope transport through the subsurface matrix flow, only; (c): considers transport through the matrix plus along preferential flow paths.

grain sizes (Vrugt et al. 2001; Durner et al. 2008; Thoma et al. 2014; Graham et al. 2018). Fitted saturated hydraulic conductivity K_s (146.34 cm/day, Table 3) is within typical ranges for sandy silt soils (Freeze and Cherry 1979; Jiang et al. 2010). Observed versus simulated Q for considering matrix flow only or matrix and preferential flow are shown in Figure S6. In addition to homogeneous conditions, multilayer scenarios were also modeled, with four layers for Ly1 and five layers for Ly2 (cf. Table S1). Modeled results were very similar to the homogeneous case (results not shown).

Comparison of LPM Application and Numerical Modeling

Seasonal periodicity of stable water contents in seepage water is met well by both approaches. For Ly2, observations are more difficult to describe (Figure 2 and 4b).

For Ly1, P_D fitted with HYDRUS-1D was lower (0.07) compared with P_D of 0.10–0.11 from LPM modeling. In contrast, for Ly2, P_D obtained from numerical modeling was slightly higher (0.85, Table 3) compared with LPM (averages 0.6–0.7, Table 2). From numerical modeling studies, Robin et al. (1983) found higher P_D-values when neglecting immobile water as a second porosity system. Similar observations were reported for comparative simulations done by Stumpp et al. (2009c) and Maraqa et al. (1997). Concerning preferential flow, for Ly1, p_{PF} found from numerical modeling (5–7%, Table 3) is slightly lower than from LPM application (average 8–13%, Table 1). For Ly2,

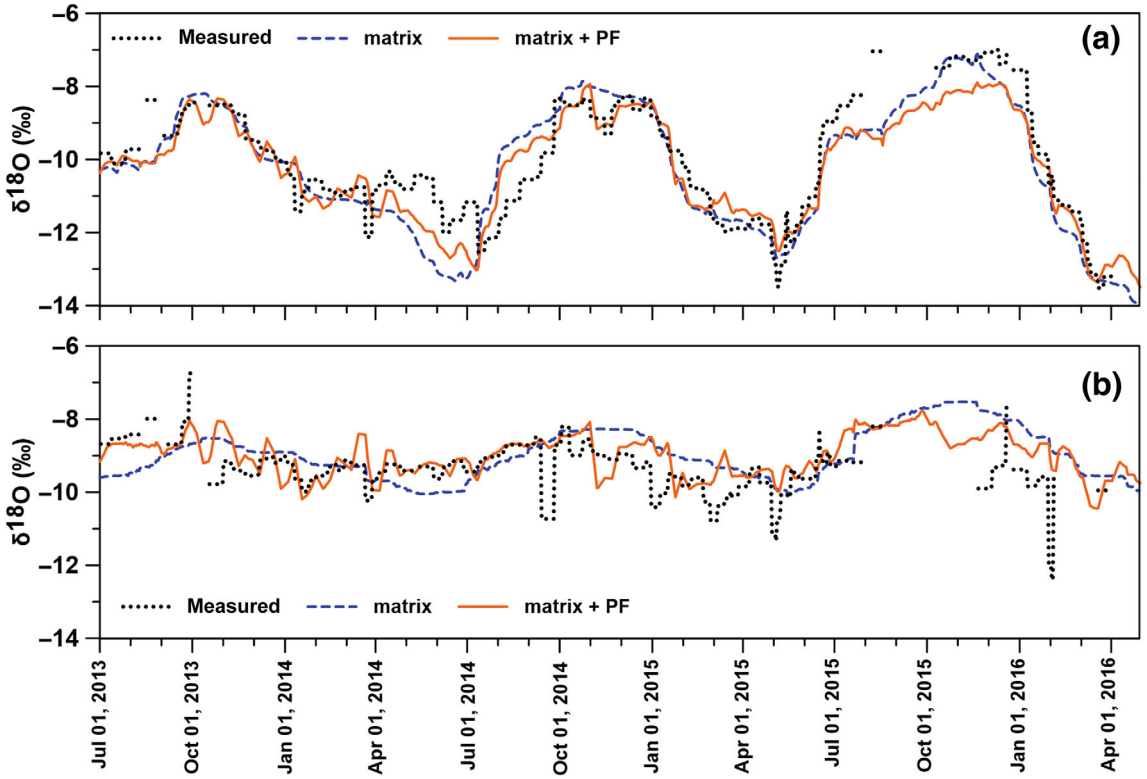

Figure 3. Measured versus modeled (HYDRUS-1D) $\delta^{18}O$ in the seepage water of Ly1 (a) and Ly2 (b); transport through the subsurface matrix and along preferential flow paths (PF).

p_{PF} found from numerical modeling (12–13%, Table 3) exceeds the LPM best fit (7–9%, Table 2).

MTT and *T* are similar for Ly1, with a somewhat lower average for *MTT* (100 days for MTT vs. 126–131 days for LPM, for the different input functions, Table 4). For Ly2, *MTT* is much lower than *T*, with 197 days in average vs. 354–361 days. Additional simulation studies with a higher saturated water content θ_s led to an increase in *MTT*, with averages of 274 days ($\theta_s = 0.4\,cm^3/cm^3$) and 342 days ($\theta_s = 0.5\,cm^3/cm^3$) (Table 4). Such higher values of θ_s (instead of the fitted values around $0.29\,cm^3/cm^3$) are also more often reported for silty soils.

Comparison of Model Concepts and Potential Improvements

Flow variation is described in a much higher temporal resolution by the numerical model (daily) than by the extended LPM (half-year). As a consequence, the degree of freedom for *T* and P_D value fitting seems higher for the extended LPM approach.

In contrast, the LPM takes an integral view within a "black box": *T* encompasses the mean transit time of soil water in total, that is, percolating (mobile) water as well as contributions of (remobilized) immobile water. Accordingly, *MTT* would only be a part of this *T*. This explains the large difference between *T* and *MTT* for Ly2.

The possible overestimation of P_D for Ly2 might be related to shortcomings in our model setup. An extension of our numerical model to a dual-porosity approach could possibly reduce deviations as well. It has the potential of describing immobile water and its influence on flow and stable water isotope transport mechanistically. However, measurements of soil water contents and/or hydraulic potential within soil, at different depths, are recommended (which were not available for this study) for model calibration, to reduce uncertainties associated with such a (more complex) approach.

The numerical model approach could also be extended by considering the uptake of water by plant roots within the soil column. Although root water uptake is not expected to alter the isotopic composition significantly (Zimmermann et al. 1967; Allison et al. 1984), it affects soil water contents during the vegetation period (Sprenger et al. 2016).

Summary and Conclusions

The extended lumped-parameter model (LPM) approach considers temporally variable flow and transport conditions. With simplified assumptions, the model addresses preferential flow and the influence of quasi-immobile water on stable water isotopes, in addition to water flow and stable water isotope transport within the subsurface matrix.

This model was applied successfully to a three-year study with two lysimeters (Ly1 and Ly2) characterized by different soil textures and the same vegetative cover (maize). Improvements were obtained in comparison to

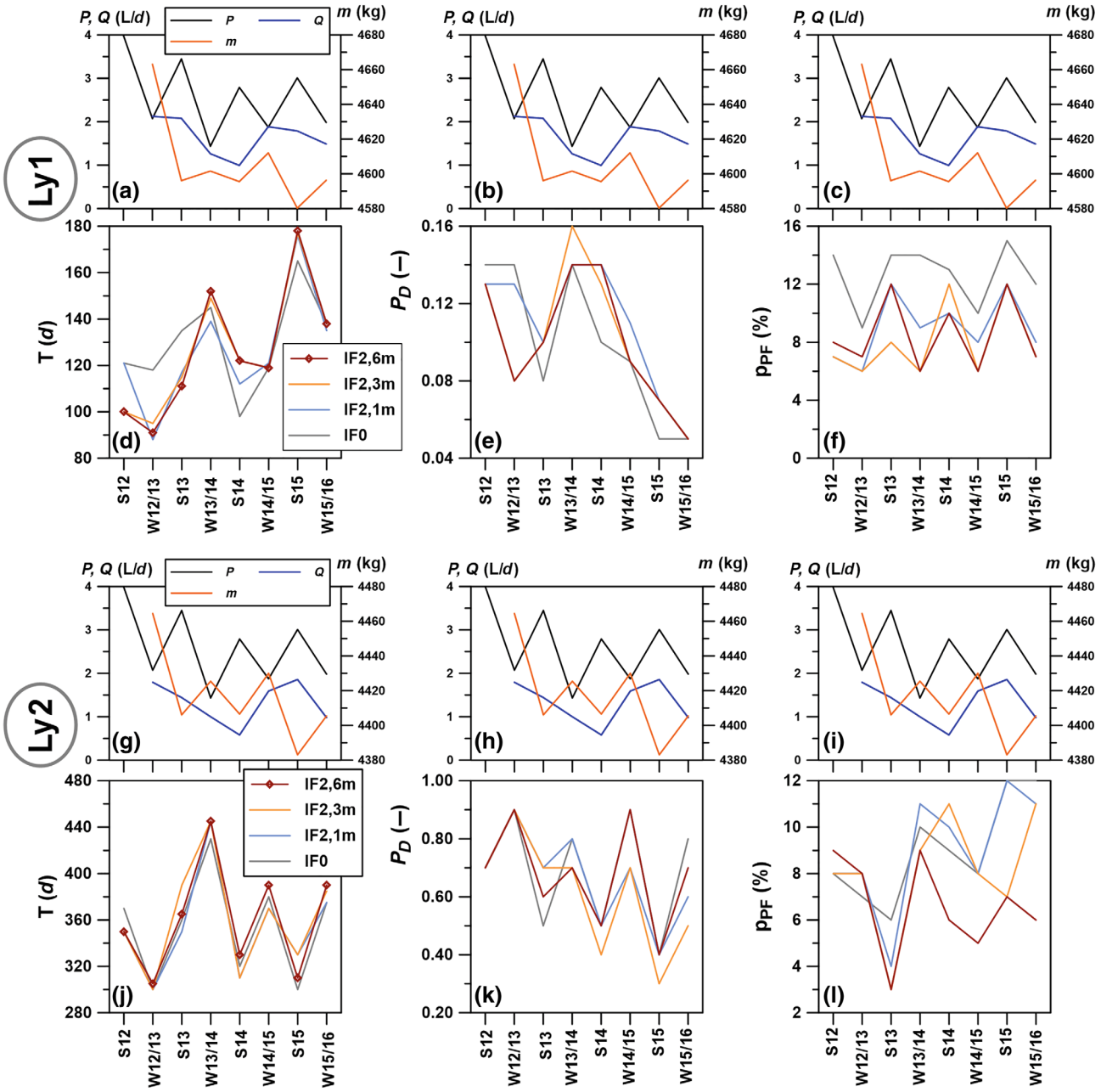

Figure 4. Temporal variation of parameters found from applying the extended lumped-parameter model (extended LPM) with different input functions IF for Ly1 (d–f) and Ly2 (j–l) (cf. Tables 1 and 2). Parameters are compared with 6-month-averages of precipitation (P), lysimeter drainage (Q), and lysimeter weight (m) (panels a–c are identical, panels g–i are identical).

"traditional" lumped-parameter modeling that considered steady-state flow. Pronounced seasonal (summer–winter) and year-to-year variations were found for mean transit time of water T, dispersion parameter P_D and portion of preferential flow p_{PF}. Measured stable water isotopes in seepage water were more difficult to explain for Ly2.

Results of the extended LPM approach were compared with results from numerical modeling of HYDRUS-1D. The latter was extended for the consideration of preferential flow and the influence of immobile water (isotopic upshift), in analogy to the extended LPM. In general, model curves from both approaches match each other. For Ly2, in addition to (slight) differences in P_D, transit times of water differed significantly (T vs. MTT). These differences cannot be fully explained: uncertainties for numerical modeling are associated, among others, with missing measurements within the soil columns, such as of water content, pressure head or stable water isotopes. As an advantage of the extended LPM approach, uncertainties of flow characterization are reduced by identifying ranges of plausible parameters as a result of temporally changing flow (and transport) conditions. A step-wise procedure is recommended, with (i) finding one set of parameters (T, P_D, and p_{PF}) for the whole simulation time (application

Table 3
Parameter Sets Fitted for Ly1 and 2 by Inverse Numerical Flow and Isotope Transport Modeling and Statistics

Depth (cm)	θ_r (cm^3/cm^3)	θ_s (cm^3/cm^3)	α (1/cm)	n (−)	K_S (cm/day)	l (−)	P_D (−)	p_{PF} (%)	T_{PF} (day)	R^2 (−)	RMSE (‰)	ME (‰)
Ly1												
0–200	0.007	0.275	0.35	1.41	6040.20	0.5	0.07	8–11	6–7	0.85	0.67	−0.14
Ly2												
0–200	0.026	0.29	0.005	1.23	146.34	0.5	0.85	12–13	5–7	0.20	0.83	−0.52

Table 4
Median Transit Time (*MTT*) Obtained by Numerical Modeling of Virtual Tracers for Ly1 und Ly2

Sub-period	S12	W12/13	S13	W13/14	S14	W14/15	S15	W15/16	Av.
Lysimeter 1									
MTT (day)	76	96	91	163	97	103	93	97	100
Lysimeter 2									
MTT (day)	199	242	223	230	187	185	176	162	197
$MTT_{0.4}$ (day)	298	335	293	304	247	254	226	222	274
$MTT_{0.5}$ (day)	393	408	350	365	299	306	267	267	342

Note: $MTT_{0.4}$ and $MTT_{0.5}$: assuming a higher saturated water content θ_s of 0.4 and 0.5 cm^3/cm^3, respectively.

of the "traditional" LPM approach) and (ii) finding temporally varying parameters for hydraulically relevant subperiods, such as seasons or vegetation periods (application of the extended LPM approach for strongly varying flow conditions). This represents a valuable tool for flow characterization, with the advantage of significantly lower data requirements compared with numerical modeling.

Acknowledgments

The authors acknowledge the Bavarian Environment Agency (Bayerisches Landesamt für Umwelt, LfU) for collecting water samples, providing field data and site-related support. The authors thank Susanne Thiemann who was involved in analyzing stable water isotopes at the laboratory of the Chair of Hydrogeology of the Technical University of Munich. We also thank the anonymous reviewers for their insightful comments that helped to greatly improve this article. Open Access funding enabled and organized by Projekt DEAL. Open Access funding enabled and organized by Projekt DEAL.

Authors' Note

Anne Imig and Fatemeh Shajari share first authorship for this publication, where Anne Imig carried out numerical modeling (HYDRUS-1D) and Fatemeh Shajari conducted lumped-parameter modeling. Co-authors supported and accompanied this modeling work by contributing to specific tasks and providing critical feedback. All authors contributed to the conception and design of the work, discussed the results, and contributed to the final manuscript.

Supporting Information

Additional supporting information may be found online in the Supporting Information section at the end of the article. Supporting Information is generally *not* peer reviewed.

Appendix S1 Supporting Information.

References

Allison, G.B., C. Barnes, C.M. Hughes, and F. Leaney. 1984. Effect of climate and vegetation on oxygen-18 and deuterium profiles in soils. In *Isotope Hydrology 1983*, ed. IAEA, 105–122. Vienna: IAEA.

Asadollahi, M., C. Stumpp, A. Rinaldo, and P. Benettin. 2020. Transport and water age dynamics in soils: A comparative study of spatially integrated and spatially explicit models. *Water Resources Research* 56, no. 3: WR025539.

Benettin, P., P. Queloz, M. Bensimon, J.J. McDonnell, and A. Rinaldo. 2019. Velocities, residence times, tracer breakthroughs in a vegetated lysimeter: A multitracer experiment. *Water Resources Research* 55, no. 1: 21–33.

Blanchoud, H., E. Moreau-Guigon, F. Farrugia, M. Chevreuil, and J.M. Mouchel. 2007. Contribution by urban and agricultural pesticide uses to water contamination at the scale of the Marne watershed. *Science of the Total Environment* 375, no. 1-3: 168–179.

Bradford, S.A., J. Simunek, M. Bettahar, M.T. Van Genuchten, and S.R. Yates. 2003. Modeling colloid attachment, straining, and exclusion in saturated porous media. *Environmental Science & Technology* 37, no. 10: 2242–2250.

Dann, R., M. Close, M. Flintoft, R. Hector, H. Barlow, S. Thomas, and G. Francis. 2009. Characterization and estimation of hydraulic properties in an alluvial gravel vadose zone. *Vadose Zone Journal* 8, no. 3: 651–663.

Demand, D., T. Blume, and M. Weiler. 2019. Spatio-temporal relevance and controls of preferential flow at the landscape

scale. *Hydrology and Earth System Sciences* 23, no. 11: 4869–4889.
Dinelli, G., C. Accinelli, A. Vicari, and P. Catizone. 2000. Comparison of the persistence of atrazine and metolachlor under field and laboratory conditions. *Journal of Agricultural and Food Chemistry* 48, no. 7: 3037–3043.
Doherty, J. 2020. Model-independent parameter estimation user manual part II: PEST utility support software. *Watermark Numerical Computing*, edn. 7, 267.
Durner, W., U. Jansen, and S.C. Iden. 2008. Effective hydraulic properties of layered soils at the lysimeter scale determined by inverse modeling. *European Journal of Soil Science* 59, no. 1: 114–124.
Einsiedl, F., P. Maloszewski, and W. Stichler. 2009. Multiple isotope approach to the determination of the natural attenuation potential of a high-alpine karst system. *Journal of Hydrology* 365, no. 1-2: 113–121.
Fetter, C.W. 1993. *Contaminant Hydrogeology*, 1st ed. New York: Macmillan Publishing Company.
Freeze, R.A., and J.A. Cherry. 1979. *Groundwater*. Englewood Cliffs: Prentice-Hall Inc.
Gazis, C., and X. Feng. 2004. A stable isotope study of soil water: Evidence for mixing and preferential flow paths. *Geoderma* 119, no. 1.2: 97–111.
Grabczak, J., K. Rózański, P. Maloszewski, and A. Zuber. 1984. Estimation of the tritium input function with the aid of stable isotopes. *Catena* 11, no. 2-3: 105–114.
Graham, S.L., M.S. Srinivasan, N. Faulkner, and S. Carrick. 2018. Soil hydraulic modeling outcomes with four parameterization methods: Comparing soil description and inverse estimation approaches. *Vadose Zone Journal* 17, no. 1: 1–10.
Groh, J., C. Stumpp, A. Lücke, T. Pütz, J. Vanderborght, and H. Vereecken. 2018. Inverse estimation of soil hydraulic and transport parameters of layered soils from water stable isotope and lysimeter data. *Vadose Zone Journal* 17, no. 1: 1–19.
Hsieh, P., J. Bahr, T. Doe, A. Flint, G. Gee, L. Gelhar, K. Solomon, M.T. van Genuchten, and S. Wheatcraft. 2001. *Conceptual Models of Flow and Transport in the Fractured Vadose Zone*. Washington, DC: The National Academies Press.
Isch, A., D. Montenach, F. Hammel, P. Ackerer, and Y. Coquet. 2019. A comparative study of water and bromide transport in a bare loam soil using lysimeters and field plots. *Water* 11: 1–25.
Jiang, S., L. Pang, G.D. Buchan, J. Šimůnek, M.J. Noonan, and M.E. Close. 2010. Modeling water flow and bacterial transport in undisturbed lysimeters under irrigations of dairy shed effluent and water using HYDRUS-1D. *Water Research* 44, no. 4: 1050–1061.
Kreft, A., and A. Zuber. 1978. On the physical meaning of the dispersion equation and its solutions for different initial and boundary conditions. *Chemical Engineering Science* 33, no. 11: 1471–1480.
Kundzewicz, Z.W., and P. Döll. 2009. Will groundwater ease freshwater stress under climate change? *Hydrological Sciences Journal* 54, no. 4: 665–675.
Leibungut, C., P. Maloszewski, and C. Külls. 2009. *Tracers in Hydrogeology*, 1st ed. Chichester, UK: Wiley-Blackwell.
Lenda, A., and A. Zuber. 1970. Tracer dispersion in groundwater experiments. In *Isotope Hydrology 1970*, ed. IAEA, 619–641. Vienna: IAEA.
Maloszewski, P., and A. Zuber. 1982. Determining the turnover time of groundwater systems with the aid of environmental tracers. 1. Models and their applicability. *Journal of Hydrology* 57, no. 3-4: 207–231.
Maloszewski, P., S. Maciejewski, C. Stumpp, W. Stichler, P. Trimborn, and D. Klotz. 2006. Modelling of water flow through typical Bavarian soils: 2 Environmental deuterium transport. *Hydrological Sciences Journal* 51, no. 2: 298–313.
Maloszewski, P., W. Stichler, A. Zuber, and D. Rank. 2002. Identifying the flow systems in a karstic-fissured-porous aquifer, the Schneealpe, Austria, by modelling of environmental ^{18}O and ^{3}H isotopes. *Journal of Hydrology* 256, no. 1-2: 48–59.
Maloszewski, P., W. Rauert, P. Trimborn, A. Herrmann, and R. Rau. 1992. Isotope hydrological study of mean transit times in an alpine basin (Wimbachtal, Germany). *Journal of Hydrology* 140, no. 1-4: 343–360.
Maraqa, M.A., R.B. Wallace, and T.C. Voice. 1997. Effects of degree of water saturation on dispersivity and immobile water in sandy soil columns. *Journal of Contaminant Hydrology* 25, no. 3-4: 199–218.
McGuire, K.J., D.R. DeWalle, and W.J. Gburek. 2002. Evaluation of mean residence time in subsurface waters using oxygen-18 fluctuations during drought conditions in the mid-Appalachians. *Journal of Hydrology* 261, no. 1-4: 132–149.
Mualem, Y. 1976. A new model for predicting the hydraulic conductivity of unsaturated porous media. *Water Resources Research* 12, no. 3: 513–522.
Radolinski, J., L. Pangle, J. Klaus, and R.D. Stewart. 2021. Testing the 'two water worlds' hypothesis under variable preferential flow conditions. *Hydrological Processes* 35, no. 6: 1–14.
Robin, M.J., K.B. Laryea, and D.E. Elrick. 1983. Hydrodynamic dispersion during absorption of water by soil: 2. Immobile water model. *Journal of Hydrology* 65, no. 4: 333–348.
Schwärzel, K., J. Šimůnek, H. Stoffregen, G. Wessolek, and M.T. van Genuchten. 2006. Estimation of the unsaturated hydraulic conductivity of peat soils. *Vadose Zone Journal* 5, no. 2: 628–640.
Shajari, F., F. Einsiedl, and A. Rein. 2020. Characterizing water flow in vegetated lysimeters with stable water isotopes and modeling. *Groundwater* 58, no. 5: 759–770.
Šimůnek, J., M.T. Van Genuchten, and M. Šejna. 2008. Development and applications of the HYDRUS and STANMOD software packages and related codes. *Vadose Zone Journal* 7, no. 2: 587–600.
Sprenger, M., S. Seeger, T. Blume, and M. Weiler. 2016. Travel times in the vadose zone: Variability in space and time. *Water Resources Research* 52, no. 8: 5727–5754.
Sprenger, M., T.H.M. Volkmann, T. Blume, and M. Weiler. 2015. Estimating flow and transport parameters in the unsaturated zone with pore water stable isotopes. *Hydrology and Earth System Sciences* 19: 2617–2635.
Stockinger, M.P., H.R. Bogena, A. Lücke, C. Stumpp, and H. Vereecken. 2019. Time variability and uncertainty in the fraction of young water in a small headwater catchment. *Hydrology and Earth System Sciences* 23, no. 10: 4333–4347.
Stumpp, C., and M.J. Hendry. 2012. Spatial and temporal dynamics of water flow and solute transport in a heterogeneous glacial till: The application of high-resolution profiles of $\delta^{18}O$ and $\delta^{2}H$ in pore waters. *Journal of Hydrology* 438-439: 203–214.
Stumpp, C., W. Stichler, M. Kandolf, and J. Šimůnek. 2012. Effects of land cover and fertilization method on water flow and solute transport in five lysimeters: A long-term study using stable water isotopes. *Vadose Zone Journal* 11, no. 1: 1–14.
Stumpp, C., P. Maloszewski, W. Stichler, and J. Fank. 2009a. Environmental isotope ($\delta^{18}O$) and hydrological data to assess water flow in unsaturated soils planted with different crops: Case study lysimeter station 'Wagna' (Austria). *Journal of Hydrology* 369, no. 1-2: 198–208.
Stumpp, C., W. Stichler, and P. Maloszewski. 2009b. Application of the environmental isotope $\delta^{18}O$ to study water flow in unsaturated soils planted with different crops: Case

study of a weighable lysimeter from the research field in Neuherberg, Germany. *Journal of Hydrology* 368, no. 1-4: 68–78.

Stumpp, C., G. Nützmann, S. Maciejewski, and P. Maloszewski. 2009c. A comparative modeling study of a dual tracer experiment in a large lysimeter under atmospheric conditions. *Journal of Hydrology* 375, no. 3-4: 566–577.

Stumpp, C., P. Maloszewski, W. Stichler, and S. Maciejewski. 2007. Quantification of the heterogeneity of the unsaturated zone based on environmental deuterium observed in lysimeter experiments. *Hydrological Sciences Journal* 52, no. 4: 748–762.

Täumer, K., H. Stoffregen, and G. Wessolek. 2006. Seasonal dynamics of preferential flow in a water repellent soil. *Vadose Zone Journal* 5, no. 1: 405–411.

Thoma, M.J., W. Barrash, M. Cardiff, J. Bradford, and J. Mead. 2014. Estimating unsaturated hydraulic functions for coarse sediment from a field-scale infiltration experiment. *Vadose Zone Journal* 13, no. 3: 1–17.

van Genuchten, M.T. 1980. A closed-form equation for predicting the hydraulic conductivity of unsaturated soils. *Soil Science Society of America Journal* 44, no. 5: 892–898.

Varis, O. 2018. Population megatrends and water management. In *Assessing Global Water Megatrends*, ed. A.K. Biswas, C. Tortajada, and P. Rohner, 41–59. Singapore: Springer Nature.

Vrba, J., and A. Richts. 2015. *The Global Map of Groundwater Vulnerability to Floods and Droughts, Explanatory Notes*. Paris, France: UNESCO, International Hydrological Programme.

Vrugt, J.A., W. Bouten, and A.H. Weerts. 2001. Information content of data for identifying soil hydraulic parameters from outflow experiments. *Soil Science Society of America Journal* 65, no. 1: 19–27.

Winton, K., and J.B. Weber. 2018. A review of field lysimeter studies to describe the environmental fate of pesticides. *Weed Technology* 10, no. 1: 202–209.

Woldeamlak, S.T., O. Batelaan, and F. De Smedt. 2007. Effects of climate change on the groundwater system in the Grote-Nete catchment, Belgium. *Hydrogeology Journal* 15, no. 5: 891–901.

WRB. 2015. Word reference base for soil resources: International soil classification system for naming soils and creating legends for soil maps – Update 2015. Rome, Italy: Food and Agriculture Organization of the United Nations, World Soi Resources Reports 106.

Zimmermann, U., D. Ehhalt, and K.O. Muennich. 1967. Soil-water movement and evapotranspiration: Changes in the isotopic composition of the water. In *Isotopes in Hydrology 1967*, ed. IAEA, 567–585. Vienna: IAEA.